Journal of Materials Chemistry

Cite this: J. Mater. Chem., 2011, 21, 2183

www.rsc.org/materials

PAPER

Oxygen ion diffusion in cation ordered/disordered $GdBaCo_2O_{5+\delta}$

David Parfitt,[a] Alexander Chroneos,*[ab] Albert Tarancón[c] and John A. Kilner[a]

Received 2nd September 2010, Accepted 22nd November 2010
DOI: 10.1039/c0jm02924f

We use molecular dynamics in conjunction with an established set of Born model potentials to examine the oxygen ion diffusion mechanism in the double perovskite $GdBaCo_2O_{5+\delta}$. We predict that the mechanism of oxygen diffusion is highly anisotropic diffusion occurring only in the Gd–O and adjacent Co–O layers. For $GdBaCo_2O_{5.5}$ the activation energy of oxygen diffusion is 0.5 eV. We investigate the effect that cation disorder of the Gd–Ba sublattice has upon the diffusivity, the anisotropy and the diffusion mechanism in $GdBaCo_2O_{5+\delta}$, which is a model system for double perovskites and other layered compounds. Cation disorder results in a reduction of the oxygen diffusivity and the appearance of diffusion along the *c*-axis of the material. Oxygen diffusion becomes effectively isotropic when the cation sublattice is disordered.

Introduction

There is active research interest for a number of oxide compositions for solid oxide fuel cell (SOFC) applications. Importantly, SOFC will become more economically viable if their operation temperature is reduced to the intermediate temperature range (500–700 °C).[1] These temperatures of operation can be inappropriate for traditional ceramic cathodes because of their high activation energy and poor catalytic activity, which result in significant electrical losses.[2] Several studies have highlighted the potential of mixed electronic–ionic (MIEC) layered oxides such as those of the Ruddlesden–Popper (RP) series ($A_{n+1}B_nO_{3n+1}$) and of the double perovskite family ($AA'B_2O_{5+\delta}$) for cathode applications in the next generation of intermediate temperature SOFC (IT-SOFC).[3–6] An example is the double perovskite $GdBaCo_2O_{5+\delta}$ where $0 \leq \delta \leq 1$ (GBCO). Due to the significant difference between the size of the two A-cations, the Ba and Gd cations do not randomly occupy the A perovskite sites but order in alternating (001) layers (Fig. 1, please refer also to the Results section).[7,8] At high temperatures, GBCO and related materials often also display considerable oxygen non-stoichiometry; this is accommodated by partial occupancy on the oxygen sublattice, with oxygen vacancies ordered in planes as reported from the results of diffraction measurements.[9,10] The effect of cation ordering on the oxygen transport properties was clearly demonstrated by Taskin *et al.*[11,12] who observed a remarkable enhancement in the oxygen chemical diffusion coefficient in cation ordered perovskite oxides by comparing the oxygen uptake behaviour of cation disordered $Gd_{0.5}Ba_{0.5}MnO_{3-\delta}$ (obtained for air-sintered samples) with its layered counterpart $GdBaMn_2O_{5+\delta}$ (obtained for pure argon-sintered samples). However, the nature of the diffusion mechanism and its correlation with cation ordering still remain unclear.

Understanding the correlation of this particular structural feature (layer ordering), present in both RP series and double perovskites, with the observed enhancement of the oxygen mass transport properties and electrochemical performance, could be of the utmost importance for opening new perspectives in cathodes for IT-SOFCs based on layered materials and, more generally, for the better understanding of the fast oxygen transport of MIEC's. In the present study, molecular dynamics (MD) was employed to investigate the mechanism and energetics of

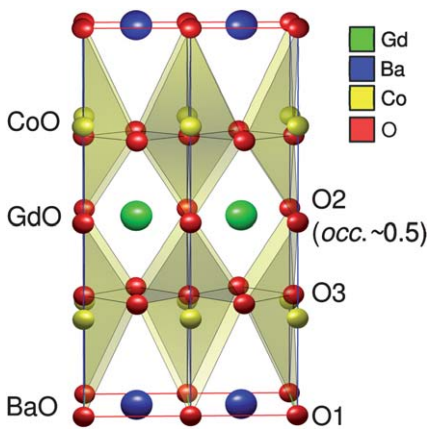

Fig. 1 The tetragonal structure of $GdBaCo_2O_{5+\delta}$ above the phase transition reported at *ca.* 700 K.[8,10] Three different oxygen sites are defined in the structure: O1 for apical oxygen in the Ba planes, O2 for apical oxygen in the Gd planes and O3 for equatorial oxygen.

[a]*Department of Materials, Imperial College London, London, SW7 2AZ, UK*
[b]*Department of Materials Science and Metallurgy, University of Cambridge, Cambridge, CB2 3QZ, UK. E-mail: ac760@cam.ac.uk*
[c]*Catalonia Institute for Energy Research (IREC), C/Josep Pla 2, edifice B2, Planta Baixa, E-08019 Barcelona, Spain*

oxygen diffusion for both ordered and disordered versions of $GdBaCo_2O_{5+\delta}$.

Methods

MD simulations were used in conjunction with the Born-like description of the ionic crystal lattice.[13] Ionic interactions were modeled with simple parameterized pair potential models. Long range Coulombic interactions were summed using the Ewald method,[14] whereas the short range interactions were described using parameterized Buckingham potentials.[15] The cutoff was at a distance of 1.05 nm and the Buckingham potential parameters were published in previous work on oxide modelling.[16–18] The efficacy of these potential parameters to describe the structure and properties of complex oxides has been demonstrated previously.[19–24] The DL POLY simulation package[25] was used for all the calculations.

Supercells of $8 \times 8 \times 4$ unit cells of the high temperature phase were used (around 5000 ions). The partial occupancy of the oxygen sites was accounted for by assigning an appropriately sized random sample of fractionally occupied oxygen sites in each layer. At each temperature the simulations were performed for 10 000 timesteps with the atoms coupled to a barostat allowing the cell parameters to change at each timestep. Thereafter 10 000 timesteps were performed under constant volume conditions effectively allowing the cell to come into equilibrium at the new volume. Production runs were restarted from these final simulations for 10 ps ensuring adequate statistical sampling. The Nose–Hoover thermostat[26,27] was used to correct the pressure and temperature. The data were analyzed using the visual molecular dynamics (VMD) package.[28]

To calculate ionic transport we monitored the mean square displacement (MSD) of ions, as a function of time, for a range of temperatures. In an N ion system the MSD of an ion i at a position $r_i(t)$ at time t with respect to its initial position $r_i(0)$ is defined by

$$\langle r_i^2(t) \rangle = \frac{1}{N} \sum_{i=1}^{N} [r_i(t) - r_i(0)]^2 \quad (1)$$

At higher temperatures oxygen ions increased their MSD with time. The oxygen diffusion coefficient, D, can be calculated from the slopes of MSD for a range of temperatures (here 800–1400 K) using[29]

$$\langle |r_i(t) - r_i(0)|^2 \rangle = 6Dt + B \quad (2)$$

where $|r_i(t) - r_i(0)|$ is the displacement of an oxygen ion from its initial position and B is an atomic displacement parameter attributed to thermal vibrations.

Results and discussion

Oxygen diffusion mechanism and energetics

Simulations were performed at 900 K starting from the *P4/mmm* ordered tetragonal structure reported for the high temperature phase (Fig. 1).[9,10] We found that at this temperature the structure presents some instabilities and there is a tendency for the O2 sites, which in the original structure are partially occupied, to absorb ions from the O3 sites to become fully occupied. This leads to a concomitant drop in the occupancy of the O3 sites.

Fig. 2(a) is the schematic representation of the calculated oxygen density profile for $GdBaCo_2O_{5.5}$ at 900 K. It is clear that the diffusion mechanism is highly anisotropic with oxygen ions migrating predominately between the O2 and O3 sites (see Fig. 1) along the *a–b* plane. We observe extensive disorder of the two oxygen sites surrounding the Gd^{3+} cations and the oxygen transport is accommodated by the O3 oxygen ions in the CoO_2 layers. The O1 oxygen ions in the Ba layers do not participate in the diffusion mechanism but they display extended displacement along the *c*-axis. This is likely due to the local stress field imposed by the movement of oxygen in the adjacent layers.

We considered $GdBaCo_2O_{5.5}$ over a wide temperature range (900–1400 K) and calculated an activation energy for oxygen diffusion of 0.5 eV. This activation energy is in excellent agreement with the previous isotopic exchange experiments, which determined an activation energy of oxygen diffusion of 0.6 eV.[30] By varying the stoichiometry slightly we calculated that the changes in this activation energy were insignificant. This indicates that the activation energy of oxygen diffusion can be relatively insensitive to small variations in the oxygen stoichiometry. Nevertheless, the diffusivities can be more sensitive to changes in the oxygen stoichiometry as they are directly related to the concentration of the diffusing oxygen vacancies. Here we observed that when the deviation from $GdBaCo_2O_{5.5}$ was significant the resulting structure was not very stable during the simulation runs. Given the flexibility of the potential parameters to describe the energetics of oxygen self-diffusion in complex oxides such as $Sr_{0.75}Y_{0.25}CoO_{2.62}$ (ref. 16 and 31), the inability of the present model to describe adequately the variation in oxygen stoichiometry in GBCO may be attributed to the structure of GBCO at high temperatures when there are significant deviations from oxygen stoichiometry.

Fig. 3 is an Arrhenius plot comparing the predicted diffusivities for $GdBaCo_2O_{5+\delta}$ with previous experimental results for $GdBaCo_2O_{5+\delta}$ and the related oxide $PrBaCo_2O_{5+\delta}$. The values of diffusivity obtained as a result of our simulations show a reasonable agreement with the experimental values reported by Taskin *et al.*[11] (after correction of the thermodynamic factor as suggested in ref. 30) and Tarancón *et al.*[30] Some of the observed

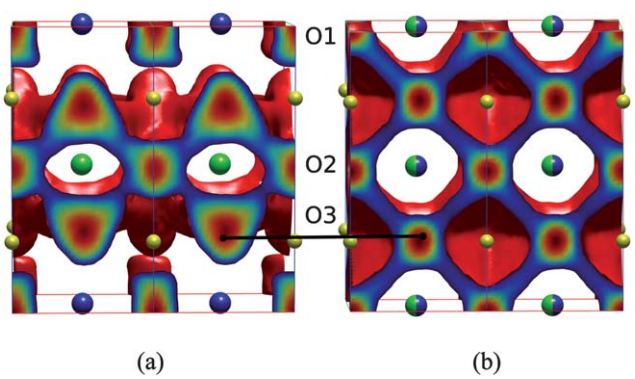

Fig. 2 (a) Calculated oxygen density profiles showing the oxygen migration pathways for (a) ordered and (b) disordered $GdBaCo_2O_{5.5}$ for $\delta = 0.5$ at 900 K.

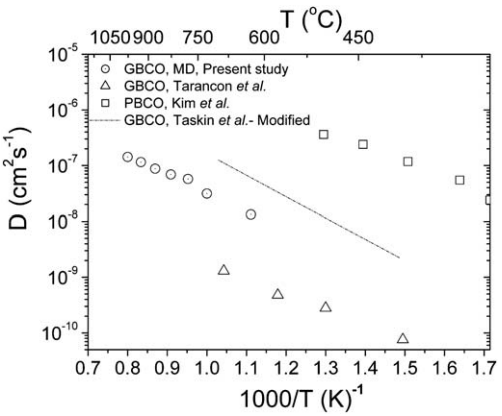

Fig. 3 Arrhenius plot of the calculated oxygen diffusivity of $GdBaCo_2O_{5+\delta}$ ($E_a = 0.5$ eV) compared to previous experimental evidence for $GdBaCo_2O_{5+\delta}$ ($E_a = 0.6$ eV of Tarancón *et al.*[30] and $E_a = 0.7$ eV of Taskin *et al.*[11]) and $PrBaCo_2O_{5+\delta}$ ($E_a = 0.48$ eV of Kim *et al.*[34]).

differences between experimental and simulated values are expected since the simulations were performed at a fixed oxygen stoichiometry of $\delta = 0.5$ while GBCO shows a strong dependence of the oxygen stoichiometry on the temperature,[10] *e.g.* falling from $\delta = 0.5$ at 300 K to $\delta = 0.15$ at 1000 K. In addition, partial disorder in the cation sublattice could also cause changes in both the activation energy and diffusivity.[32] Recent static atomistic simulations by Seymour *et al.*[33] predict a cation disorder energy of 1.25 eV per defect (for a Gd at a Ba site and a Ba at a Gd site) in orthorhombic $GdBaCo_2O_{5.5}$. Interestingly, the diffusivities of all the $GdBaCo_2O_{5+\delta}$ investigations considered here are considerably lower compared to the diffusivities of Kim *et al.*[34] for $PrBaCo_2O_{5+\delta}$.

Effect of cation disorder

We examine the oxygen diffusion mechanism and also the effect of disorder upon the cation ion sublattice. In the previous simulations we have assumed that the cation sublattice is fully ordered, in a real material, however, there will be a level of exchange between the Gd with Ba cations likely due to different synthesis routes and thermal history before operation. This expected A-site cation exchange has not been studied yet in ordered double perovskites of this family. In order to better understand the ionic conduction in these materials, experimental quantification of this disorder should be the matter of study in the future. From a simulation point of view we quantify this with a parameter f that represents the probability of finding a Gd ion on a Ba site,

$$f = \frac{[Gd_{Ba}]}{[Gd_{Ba}] + [Gd_{Gd}]} \quad (3)$$

where $[M_N]$ represents the concentration of M ions on an N site. This parameter varies between 0 and 1, both of which represent the fully ordered case (although the limit $f = 1$ represents the case of the Gd 'sites' in reality becoming Ba 'sites'); the fully disordered case, where there is a 50% probability of either site being occupied by a Gd or Ba ion, is given by $f = 0.5$.

For our simulations we created initial structures with a given level of cation disorder by exchanging a given fraction of Gd ions with Ba ions. This does impose a specific ordering of the cation disordered defects within the periodic repeat unit of the simulation cell, and there may be variations in physical quantities as a result. We maintain, however, that for a sufficiently large cell, these will be small and that the overall trend as a function of cation disorder will be evident. These simulations were run at 900 K and with $\delta = 0.5$.

In Fig. 2(b) we show the effect of cation disorder upon the oxygen diffusion mechanism. The data are plotted for the same effective unit cell as the ordered case, although in fact there will be a random distribution of cations over these sites. We see that the formation of cation disordered defects leads to migration pathways along the *c*-axis; oxygen ions are able to migrate around the Gd_{Ba}' (using the Kröger–Vink notation) defects to cross between adjacent Gd layers within the material. To examine the relationship between diffusion and the degree of cation disorder, we calculated the diffusivities along the *c*-axis and in the *a*–*b* plane. These simulations require long running times, ~4 ns, as the oxygen ions can move between sites along the *c*-axis (interstitial to interstitial, for example) and therefore at short times the mean displacement along the *c*-axis rises rapidly. At long timescales, however, as the diffusion is limited by the movement of ions along the *a*–*b* plane, we see a drop in the diffusion rate along the *c*-axis.

Fig. 4 shows a plot of the calculated ratio between the diffusion along the *c*-axis and in the *a*–*b* plane. As noted, in the perfectly ordered case there is no diffusion along the *c*-axis and therefore the ratio is zero. As the disorder increases the ratio rises until in the perfectly disordered case there is isotropic diffusion along each axis. The graph is symmetrical about $f = 0.5$ as the Gd and Ba sites are crystallographically identical. In Fig. 4 we also plot the net diffusivity for the material, this drops as the level of disorder is increased reaching a level approximately a third of the perfectly ordered case.

The change in diffusivity shown in Fig. 4 is remarkable, and in some ways counterintuitive, in that the cation ordered lattice ($GdBaCo_2O_{5+\delta}$) has a higher diffusivity than the cation

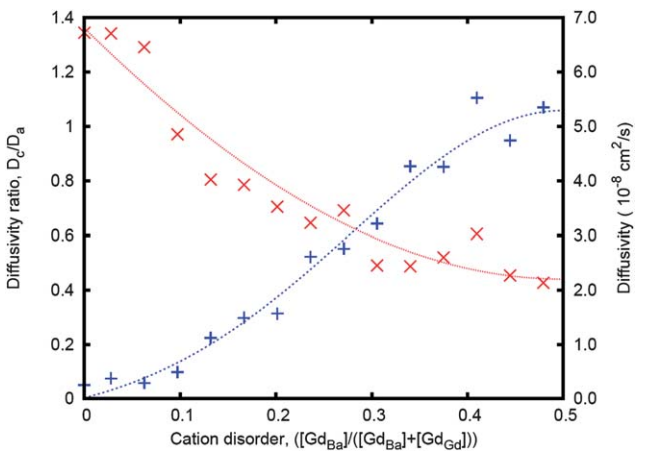

Fig. 4 The ratio of diffusivities D_c/D_a (+, blue line) along the *a*- and *c*-axis as a function of cation disorder for $\delta = 0.5$ at 1200 K. The diffusivity values (×, red line) as a function of cation disorder are also presented.

disordered lattice ($Gd_{0.5}Ba_{0.5}CoO_{3-\delta}$). Normally one would expect that the order on the oxygen sublattice would follow that on the cation lattice. This is indeed so for GBCO at lower temperatures but above a temperature of *ca.* 500 °C the anion sublattice is disordered and the lattice oxygen in the CoO and GdO layers increases its mobility.[10] This phenomenon has been remarked upon by Norby[35] who has examined the phenomenon of linked cation and anion order. His conclusion is that although conventional wisdom would suggest avoiding cation ordered structures as oxide ion conductors, there are materials with cation order and anion disorder that show high mobility for the oxygen atoms. The rationale for this is that in the disordered state, which in this case would be written as the perovskite $Gd_{0.5}Ba_{0.5}CoO_{3-\delta}$, defect trapping can occur between the oxygen vacancies and the Ba (in a Gd site) antisite atom, hence lowering the measured diffusivity.

Conclusions

We report that the oxygen self-diffusion in $GdBaCo_2O_{5+\delta}$ is strongly dependent upon the cation disorder. This is the first visualization of the effect of cation disorder on the diffusion pathway of oxygen ions in $GdBaCo_2O_{5+\delta}$. For ordered $GdBaCo_2O_{5.5}$ we predict a highly anisotropic oxygen transport mechanism along the *a–b* plane with an activation energy of diffusion of 0.5 eV in the temperature range 800–1400 K. Disorder on the cation sublattice has two effects, firstly a drop in the total oxygen diffusivity of the material and secondly the appearance of diffusion along the *c*-axis of the material, reaching effectively isotropic diffusion in the fully disordered $f = 0.5$ case. It is interesting that predictions suggest that the levels and nature of disorder and therefore diffusion in GBCO (and likely related materials) will be strongly influenced by the levels of cation disorder and therefore sample preparation and thermal history could become important parameters in understanding the experimental data. In future computational work the effect of charge transfer, cobalt spin state and the binding of vacancies with A cations (host or dopant) will be assessed in detail.

Acknowledgements

AC and JAK acknowledge support from EP/F009720/1 "New Research Directions for Solid Oxide Fuel Cell Science and Engineering". AT would like to thank the financial support of the *Ramon y Cajal* postdoctoral program and Consolider MULTICAT project (CDS-2009-00050) of the Spanish Ministry of Science and Innovation as well as the support from the "Generalitat de Catalunya" (Advanced Materials for Energy Network, XaRMAE, 2009-SGR-440). Computing resources were provided by the HPC facility of Imperial College London.

References

1 N. P. Brandon, S. Skinner and B. C. H. Steele, *Annu. Rev. Mater. Res.*, 2003, **33**, 183.
2 J. Fleig, *Annu. Rev. Mater. Res.*, 2003, **33**, 361.
3 S. J. Skinner, *Int. J. Inorg. Mater.*, 2001, **3**, 113.
4 Z. Shao, S. M. Haile, J. Ahn, P. D. Ronney, Z. Zhan and S. A. Barnett, *Nature*, 2005, **435**, 795.
5 S. B. Adler, *Solid State Ionics*, 1998, **111**, 125.
6 A. Tarancón, M. Burriel, J. Santiso, S. J. Skinner and J. A. Kilner, *J. Mater. Chem.*, 2010, **20**, 3799.
7 A. Maignan, C. Martin, D. Pelloquin, N. Nguyen and B. Raveau, *J. Solid State Chem.*, 1999, **142**, 247.
8 C. Frontera, J. L. Garcia-Muñoz, A. Llobet and M. A. G. Aranda, *Phys. Rev. B: Condens. Matter Mater. Phys.*, 2002, **65**, 180405.
9 S. Streule, A. Podlesnyak, D. Sheptyakov, E. Pomjakushina, M. Stingaciu, K. Conder, M. Medarde, M. V. Patrakeev, I. A. Leonidov, V. L. Kozhevnikov and J. Mesot, *Phys. Rev. B: Condens. Matter Mater. Phys.*, 2006, **73**, 094203.
10 A. Tarancón, D. Marrero-López, J. Peña-Martinez, J. C. Ruiz-Morales and P. Núñez, *Solid State Ionics*, 2008, **179**, 611.
11 A. A. Taskin, A. N. Lavrov and Y. Ando, *Appl. Phys. Lett.*, 2005, **86**, 91910.
12 A. A. Taskin, A. N. Lavrov and Y. Ando, *Prog. Solid State Chem.*, 2007, **35**, 481.
13 M. Born and J. E. Mayer, *Z. Phys.*, 1932, **75**, 1.
14 P. P. Ewald, *Ann. Phys. (Paris, Fr.)*, 1921, **64**, 253.
15 R. A. Buckingham, *Proc. R. Soc. London, Ser. A*, 1938, **168**, 264.
16 D. Rupasov, A. Chroneos, D. Parfitt, J. A. Kilner, R. W. Grimes, S. Ya. Istomin and E. V. Antipov, *Phys. Rev. B: Condens. Matter Mater. Phys.*, 2009, **79**, 172102.
17 A. Chroneos, D. Parfitt, J. A. Kilner and R. W. Grimes, *J. Mater. Chem.*, 2010, **20**, 266.
18 D. Parfitt, A. Chroneos, J. A. Kilner and R. W. Grimes, *Phys. Chem. Chem. Phys.*, 2010, **12**, 6834.
19 R. A. De Souza and J. Maier, *Phys. Chem. Chem. Phys.*, 2003, **5**, 740.
20 A. Chroneos, K. Desai, S. E. Redfern, M. O. Zacate and R. W. Grimes, *J. Mater. Sci.*, 2006, **41**, 675.
21 C. A. J. Fisher and M. S. Islam, *J. Mater. Chem.*, 2005, **15**, 3200.
22 M. R. Levy, C. R. Stanek, A. Chroneos and R. W. Grimes, *Solid State Sci.*, 2007, **9**, 588.
23 A. Chroneos, R. V. Vovk, I. L. Goulatis and L. I. Goulatis, *J. Alloys Compd.*, 2010, **494**, 190.
24 A. Kushima, D. Parfitt, A. Chroneos, B. Yildiz, J. A. Kilner and R. W. Grimes, *Phys. Chem. Chem. Phys.*, 2011, DOI: 10.1039/c0cp01603a.
25 W. Smith and I. Todorov, *The DLPOLY 3.0 User Manual*, Daresbury Laboratory, UK.
26 S. Nose, *J. Chem. Phys.*, 1984, **81**, 511.
27 W. G. Hoover, *Phys. Rev. A: At., Mol., Opt. Phys.*, 1985, **31**, 1695.
28 W. Humphrey, A. Dalke and K. Schulten, *J. Mol. Graphics*, 1996, **14**, 33.
29 M. J. Gillan, *Physica B (Amsterdam)*, 1985, **131**, 157.
30 A. Tarancón, S. J. Skinner, R. J. Chater, F. Hernandez-Ramirez and J. A. Kilner, *J. Mater. Chem.*, 2007, **17**, 3175.
31 D. P. Rupasov, A. V. Berenov, J. A. Kilner, S. Ya. Istomin, and E. V. Antipov, *Solid State Ionics*, under review.
32 J. H. Kim and A. Manthiram, *J. Electrochem. Soc.*, 2008, **155**, B385.
33 I. Seymour, A. Chroneos, J. A. Kilner, and R. W. Grimes, unpublished results.
34 G. Kim, S. Wang, A. J. Jacobson, L. Reimus, P. Brodersen and C. A. Mims, *J. Mater. Chem.*, 2007, **17**, 2500.
35 T. Norby, *J. Mater. Chem.*, 2001, **11**, 11.

